

Statistics of waves propagating in a random medium

Eugene Kogan, Moshe Kaveh, Rene Baumgartner, and Richard Berkovits

*The Jack and Pearl Resnick Institute of Advanced Technology, Department of Physics, Bar-Ilan University
Ramat-Gan 52900, Israel*

(Received 20 October 1992; revised manuscript received 3 May 1993)

The statistics of coherent radiation propagating in a random medium is analyzed in the framework of diagrammatic techniques. The distribution function for radiation intensity is calculated and it is shown that only for small values of intensity is the distribution function a simple exponential, as predicted by Rayleigh statistics. For larger values of intensity, the distribution function differs drastically from a simple exponential, and exhibits the asymptotic behavior of a stretched exponential. The results obtained are confirmed by numerical simulations.

The interest in problems of transport through disordered media was revived after the discovery of strong mesoscopic fluctuations in such systems. It was found,^{1,2} that the variance of the dimensionless conductance g for electrons is much larger than would follow from classical consideration and has a universal value. This phenomenon is known as UCF (universal conductance fluctuations). Later, it was demonstrated that UCF exist also for the propagation of classical waves (e.g., light) through disordered systems.³ In contrast to electronic measurements, which can measure only the conductance of a system, light experiments have the advantage of being able to measure the angular transmission coefficients for an experimental realization. The angular transmission coefficient t_{ab} is defined as the ratio of the energy carried away by the transmitted wave with the transverse wave vector \mathbf{q}_b to the energy of the incident wave with the transverse wave vector \mathbf{q}_a . The total transmission due to an incoming wave of transverse wave vector \mathbf{q}_a is $t_a = \sum_b t_{ab}$. The conductance, which is the sum of the total transmission from all incident angles, is given by $g = \sum_{a,b} t_{ab}$.

Soon after the discovery of conductance fluctuations the question of calculating not only the variance but the whole distribution function of the conductance was solved (Ref. 4 and references therein). A natural question that immediately arises is whether one could also calculate the distribution function of the total and angular transmission coefficient. The latter problem, as we shall see, is closely connected with the problem of calculating the radiation intensity statistics in a disordered medium. It is especially timely, since experiments are now under way,⁵ which probe the statistics of microwave radiation in disordered media.

In this paper we analyze the problem of statistics in the framework of diagrammatic techniques. We obtain an equation, which expresses the distribution function through the connected diagram contributions only. On the basis of this equation the "topological" approximations are formulated. We show that Rayleigh statistics

for the angular transmission coefficients (intensity) corresponds to the first-order approximation (the same approximation applied to conductance and the total transmission coefficient gives no fluctuations at all). We explicitly calculate the statistics of the angular transmission coefficients (intensity) in the second-order approximation, which gives the Gaussian distribution function for conductance (as well as for the total transmission coefficient).

It is well known that Rayleigh statistics for the angular transmission coefficient t_{ab} are represented by the following distribution function $P_R(t_{ab})$:

$$P_R(t_{ab}) = \frac{1}{\langle t_{ab} \rangle} \exp\left(-\frac{t_{ab}}{\langle t_{ab} \rangle}\right), \quad (1)$$

which corresponds to the equation for the moments:

$$\langle t_{ab}^n \rangle = n! \langle t_{ab} \rangle^n. \quad (2)$$

This statistic is in fact the manifestation of the central limit theorem. If we suppose the field of the wave radiated in a given direction to be the sum of large number of independent random complex terms ("contributions from different uncorrelated trajectories") than the energy carried by this wave, which is proportional to the square of the modulus of the field, is distributed according to the simple exponential law, given by Eq. (1). But it is well known that if we take into account the wave nature of the carriers, there will be interference between different trajectories. It is this interference that leads to strong non-classical "mesoscopic" fluctuations. We want to study how this interference influences the statistics, using the framework of traditional diagrammatic techniques.

First let us recall how Rayleigh statistics are obtained in this framework.⁶ In the diagrammatic representation, $\langle t_{ab} \rangle$ is given by the diagrams with a pair of wave propagators G_{ab}^R and G_{ab}^A summed with respect to all possible interconnections by impurity scattering lines. The n th moment $\langle t_{ab}^n \rangle$ is given by the set of diagrams with n propagators G_{ab}^R and n propagators G_{ab}^A (see Fig. 1). For our

consideration the following property of diagrams are important: if the diagram consists of several disconnected parts, then the contribution of that diagram is equal to the product of the contributions of all disconnected parts. Therefore, if we consider for $\langle t_{ab}^n \rangle$ only the diagrams consisting of n disconnected parts, each part being the set of diagrams with a pair of propagators (advanced and retarded), we immediately obtain Eq. (2). The multiplier $n!$, which appears in the n th moment, is of combinatorial origin; it is simply the number of possible pairings between propagators.

The generalization of this result is straightforward. An arbitrary diagram for $\langle t_{ab}^n \rangle$ is, generally speaking, disconnected and consists of several connected parts (see Fig.

2), i.e., it has m_1 parts with one pair of propagators (advanced and retarded one), m_2 parts with two pairs and so on up to n pairs (the connected diagrams where the number of advanced propagators does not coincide with the number of retarded propagators would give a contribution of higher order with respect to the small parameter $\exp(-L/\ell)$, where ℓ is a mean free path and L is a sample thickness, which may be neglected). So we can classify all the diagrams according to their topology, which is given by the numbers $\{m_1, \dots, m_n\}$, and the sum of all diagrams can be written down in the following way:

$$\langle t_{ab}^n \rangle = n! M_n, \tag{3}$$

where

$$M_n = \sum_{m_1+2m_2+\dots+nm_n=n} P(m_1, m_2, \dots, m_n) \langle t_{ab} \rangle_c^{m_1} \langle t_{ab}^2 \rangle_c^{m_2} \dots \langle t_{ab}^n \rangle_c^{m_n}; \tag{4}$$

the connected diagram contribution $\langle t_{ab}^i \rangle_c$ is the sum of all connected diagrams with i pairs of propagators and

$$P(m_1, m_2, \dots, m_n) = \frac{n!}{(1!)^{m_1} (2!)^{m_2} \dots (n!)^{m_n} m_1! m_2! \dots m_n!} \tag{5}$$

is the number of partitions of n different objects into m_1 groups of one object, m_2 groups of two objects and so on. The summation in Eq. (4) is with respect to all possible non-negative integers satisfying the given equation. A single term in the sum in Eq. (4) gives the contribution from all the diagrams with the topology given by the numbers $\{m_1, \dots, m_n\}$, and the multipliers $n!$ and $P(m_1, m_2, \dots, m_n)$ are of purely combinatorial origin resulting from the number of ways we can couple propagators, and the latter is the number of partitions of n

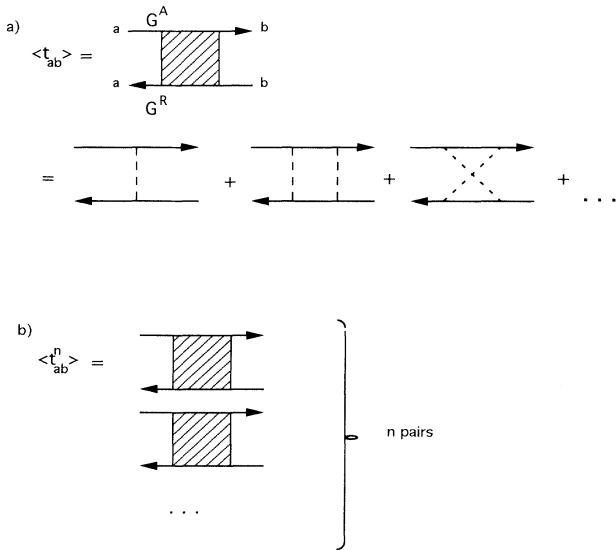


FIG. 1. Feynman diagrams used in the calculation of the angular transmission coefficient moments. (a) The averaged angular transmission coefficient. (b) The n th moment in the Rayleigh approximation.

pairs between connected diagrams.

The distribution function $P(t_{ab})$ is connected to its moments in the usual way:

$$P(t_{ab}) = \int_{-\infty}^{\infty} \exp(i\xi t_{ab}) \sum_{n=0}^{\infty} \frac{(-i\xi)^n}{n!} \langle t_{ab}^n \rangle \frac{d\xi}{2\pi}. \tag{6}$$

Using the integral representation for $n!$,

$$n! = \int_0^{\infty} du u^n \exp(-u), \tag{7}$$

for the distribution function $P(t_{ab})$ we have, changing the integration variable to $\zeta = \xi u$,

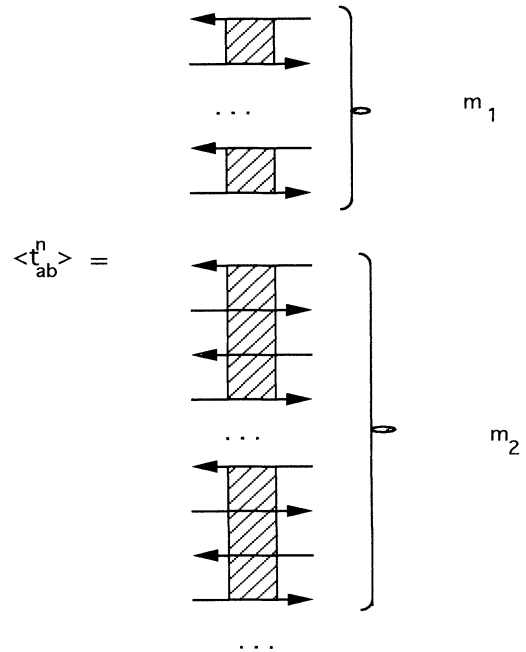


FIG. 2. Feynman diagrams used in the calculation of the angular transmission coefficients moments where all possible connected parts are taken in account.

$$P(t_{ab}) = \int_{-\infty}^{\infty} \exp(i\zeta t_{ab}/u) \int_0^{\infty} du \sum_{n=0}^{\infty} \frac{(-i\zeta)^n}{n!} M_n \frac{1}{u} \exp(-u) \frac{d\zeta}{2\pi}. \quad (8)$$

From Eq. (5) follows

$$\sum_{n=0}^{\infty} \frac{(-i\zeta)^n}{n!} M_n = \sum_{m_1=0}^{\infty} \frac{(-i\zeta)^{m_1}}{m_1!} \left(\frac{\langle t_{ab} \rangle_c}{1!} \right)^{m_1} \sum_{m_2=0}^{\infty} \frac{(-i\zeta)^{m_2}}{m_2!} \left(\frac{\langle t_{ab}^2 \rangle_c}{2!} \right)^{m_2} \dots = \exp \left(\sum_{n=1}^{\infty} \frac{(-i\zeta)^n}{n!} \langle t_{ab}^n \rangle_c \right). \quad (9)$$

Supposing the absolute continuity of the integrals in Eq. (8) and changing the integration variable $v = t_{ab}/u$ in Eq. (8), we finally obtain

$$P(t_{ab}) = \int_0^{\infty} dv \tilde{P}(v) \frac{1}{v} \exp\left(-\frac{t_{ab}}{v}\right), \quad (10)$$

where we have introduced an auxiliary function $\tilde{P}(v)$ given by the equation

$$\tilde{P}(v) = \int_{-\infty}^{\infty} \exp(i\zeta v) \exp\left(\sum_{n=1}^{\infty} \frac{(-i\zeta)^n}{n!} \langle t_{ab}^n \rangle_c\right) \frac{d\zeta}{2\pi}. \quad (11)$$

The distribution function (10) can be described as the Rayleigh distribution function but with some effective averaged value, which in turn fluctuates around the real averaged value. We can also change the order of integration in Eq. (10) and perform the integration with respect to dv . Then Eq. (11) takes the form:

$$P(t_{ab}) = \int_{-\infty}^{\infty} \exp\left(\sum_{n=1}^{\infty} \frac{(-i\zeta)^n}{n!} \langle t_{ab}^n \rangle_c\right) \times K_0\left(2\sqrt{i\zeta t_{ab}}\right) \frac{d\zeta}{\pi}, \quad (12)$$

where K_0 is the modified Bessel function. This equation is less convenient for application than Eq. (10); we show it in order to underline the fact that the expansion with respect to connected diagrams differs from the expansion with respect to cumulants.

We have obtained an exact equation that expresses the distribution function in terms of the connected diagrams contribution only. Of course, that by itself does not solve the problem of finding the distribution function as the expression of the one-particle Green's function through the irreducible diagrams (self-energy), and does not solve the problem of finding the Green's function. However, the approximations for the self-energy are simpler than the approximations for the Green's function itself. Therefore, we may hope to get simple reasonable approximations for the auxiliary function $\tilde{P}(v)$. We propose one such approximation. First we notice that, if we retain in the sum $\sum_{n=1}^{\infty} \frac{(-i\zeta)^n}{n!} \langle t_{ab}^n \rangle_c$ only the first term, we immediately get Rayleigh statistics from Eq. (10). This suggests that in an approximation of the order m one should take into account only m types of connected diagrams; that is, one should retain in the sum $\sum_{n=1}^{\infty} \frac{(-i\zeta)^n}{n!} \langle t_{ab}^n \rangle_c$ only the first m terms. Hence we obtain the distribution function in terms of $\{\langle t_{ab} \rangle_c, \langle t_{ab}^2 \rangle_c, \dots, \langle t_{ab}^m \rangle_c\}$, which should be treated in our theory as m input parameters. Because we classify the diagrams only according to their

topological properties, it is natural to refer to such an approximation as a "topological" one. Here an important point should be mentioned. To procure the convergence of the integration with respect to $d\zeta$ in Eq. (10) for the approximation of the order m , there should be a "correct" sign before the highest even power of ζ (minus) in the truncated exponent. As long as the sign is negative, we can proceed with our treatment. On the other hand, if the sign is positive, we should rewrite Eqs. (10) and (11) using a more general transformation than Eq. (7). In the Appendix we describe this more general procedure. The results in the appendix [Eqs. (A3) and (A4)] contain Eqs. (10) and (11) as a particular case but can also be applied for the case in which a "wrong" sign appears before the highest even power of ζ in the truncated exponent.

From a mathematical point of view we expressed the broad distribution function $P(t_{ab})$ through an auxiliary function $\tilde{P}(v)$ for which the second cumulant is much smaller than the first cumulant (see discussion latter). Hence, $\tilde{P}(v)$ describes a narrow distribution. In the traditional approach only the first cumulant is considered, i.e., $\tilde{P}(v) = \delta(v)$. In taking into account additional cumulants, we take into account the finite width of the auxiliary distribution. As can be seen in Eq. (10), when $t_{ab}/\langle t_{ab} \rangle$ is not too large, the main contribution to the integral comes from the maximum of $\tilde{P}(v)$, which can be well described from the knowledge of a few cumulants. Once $t_{ab}/\langle t_{ab} \rangle \rightarrow \infty$ the main contribution is from the tails of $\tilde{P}(v)$ and any truncation approximation is dubious (in particular the tail behavior will depend on the dimensionality, which does not appear explicitly in our approximation).

We shall present explicit results for the second-order approximation. In this approximation the distribution function is determined by $\langle t_{ab} \rangle_c$ and $\langle t_{ab}^2 \rangle_c$, which can be easily calculated; the first is determined mainly by ladder diagrams, the second by Hikami box diagrams; the latter were calculated in Ref. 3 (and we also have the "correct" sign of $\langle t_{ab}^2 \rangle_c$). Equation (10), however, can be viewed from another point of view. The system of equations (3) should be understood as expressing the connected diagram contributions through the moments. For example, the first two equations give

$$\langle t_{ab} \rangle_c = \langle t_{ab} \rangle, \quad (13)$$

$$\langle t_{ab}^2 \rangle_c = \langle t_{ab}^2 \rangle / 2 - \langle t_{ab} \rangle^2.$$

Roughly speaking, we make an expansion of the distribution function near Rayleigh statistics and restore the

distribution function on the basis of only two known moments,

$$P(t_{ab}) \sim \int_0^\infty dv \exp\left[-\frac{(v - \langle t_{ab} \rangle)^2}{2\langle t_{ab}^2 \rangle_c}\right] \frac{1}{v} \exp\left(-\frac{t_{ab}}{v}\right), \quad (14)$$

and Eq. (3) in this approximation can be written in the form

$$\begin{aligned} \langle t_{ab}^n \rangle &= \langle t_{ab} \rangle^n \sum_{m=0}^{[n/2]} \frac{(n!)^2}{m!(n-2m)!} (2\Delta)^{-2m} \\ &= n! \left(\frac{\langle t_{ab} \rangle}{2i\Delta}\right)^n H_n(i\Delta), \end{aligned} \quad (15)$$

where $\Delta^2 \equiv \langle t_{ab} \rangle^2 / 2\langle t_{ab}^2 \rangle_c$ and H_n is the Hermite polynomial. (In the general case, we can express the distribution function through the m known moments.)

To check the validity of the theory proposed, we have performed numerical simulations based on a widely used model by Edrei *et al.*¹¹ A wide ($W \gg L$) two-dimensional sample was used. The sample length was $L = 6b$ and width $W = 100b$, where b is the averaged distance between the point scatterers. Since in our particular realization the scatterers were chosen to be relatively strong, the mean free path $l \sim b$. The wave length of the incoming wave is $\lambda = 0.01234b$, therefore, $kl \sim 500$. The intensity and its first 15 moments on the outgoing face were averaged over 864 different realizations and over the different 100 outgoing bonds in each realization. The results are represented in Fig. 3. The full line corresponds to Eq. (15), the dotted line to Rayleigh statistics and the (+) symbols to the results of the numerical simulation. A good fit is obtained up to the eighth moment, where only two fitting parameters ($\langle t_{ab} \rangle$, and $\langle t_{ab}^2 \rangle_c$) were used. The simulation results for higher moments fall even below what is expected from Rayleigh statistics. This is due to the fact that high-order moments are strongly influenced by rare realizations in which the averaged transmission is very high. Since we have used only a limited number

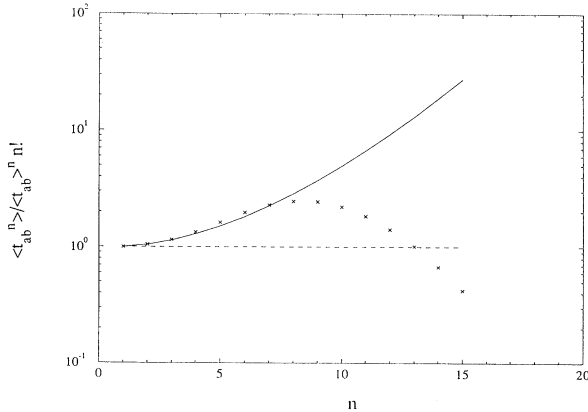


FIG. 3. Moments of the angular transmission coefficient. The full line corresponds to Eq. (15), the dotted line to Rayleigh statistics, and the (+) symbols to the results of the numerical simulation.

of realizations, discrepancies for high moments are to be expected.

The functional dependence of the distribution function given by Eq. (14) is determined in fact by a single parameter Δ . The term $\langle t_{ab}^2 \rangle_c$ being known,³ we get $\Delta^2 \sim g_0$, where g_0 is the classical conductance. We are considering the “metallic phase,” i.e., $g_0 \gg 1$. That means that in the exponent in the Eq. (14) there is a large parameter, and the integral can be calculated by the steepest descent method. We consider explicitly the following particular cases.

(1) $t_{ab} / \langle t_{ab} \rangle \ll \Delta$, where we get

$$P(t_{ab}) = P_R(t_{ab}). \quad (16)$$

It is interesting that our distribution function has a weak singularity: when t_{ab} goes to zero, $P(t_{ab}) \sim -\ln t_{ab}$; we cannot say whether this is a real effect or an artifact due to the approximations made. In any event this singularity manifests itself only for extremely low values of the argument $t_{ab} / \langle t_{ab} \rangle < \exp(-\exp \Delta^2)$.

(2) $\Delta < t_{ab} / \langle t_{ab} \rangle \ll \Delta^2$, where we can get an expansion for $\ln P(t_{ab})$ in powers of the parameter $\tilde{t} = t_{ab} / \langle t_{ab} \rangle \Delta^2$:⁸

$$\ln P(t_{ab}) = -\frac{t_{ab}}{\langle t_{ab} \rangle} \left[1 - \frac{\tilde{t}}{4} + \frac{\tilde{t}^2}{4} + \dots \right]. \quad (17)$$

(3) $t / \langle t \rangle \gg \Delta^2$, where we get an asymptotic expansion for $\ln P(t_{ab})$ in inverse powers of \tilde{t} :

$$\ln P(t_{ab}) = -\left(\frac{t_{ab}\Delta}{\langle t_{ab} \rangle}\right)^{2/3} \left[\frac{3}{4^{1/3}} - \left(\frac{4}{\tilde{t}}\right)^{1/3} + \frac{1}{(\tilde{t})^{2/3}} + \dots \right]. \quad (18)$$

We see that we get Rayleigh statistics only for $t / \langle t \rangle \ll \sqrt{g}$; outside this region the distribution function greatly exceeds P_R . In particular for $t_{ab} / \langle t_{ab} \rangle \gg g$, the distribution function has the form of a stretched exponential:

$$P(t_{ab}) \sim \exp\left[-\frac{3 t_{ab}^{2/3}}{2\langle t_{ab}^2 \rangle_c^{1/3}}\right]. \quad (19)$$

The angular transmission coefficient gives us the intensity of radiation in a given direction. Exactly the same line of reasoning that led to Eq. (14) can be applied if we are interested in the statistics of the intensity at a given point. (Statistics obtained depends only on the topology of the diagrams that are taken into account. Hence, it is not important whether the loose ends of the diagrams are marked by momentum or coordinate.) Therefore, the distribution function of the intensity $P(I)$ is analogous to Eq. (14):

$$P(I) \sim \int_0^\infty dv \exp\left[-\frac{(v - \langle I \rangle)^2}{2\langle I^2 \rangle_c}\right] \frac{1}{v} \exp\left(-\frac{I}{v}\right), \quad (20)$$

where $\langle I^2 \rangle_c = \langle I^2 \rangle / 2 - \langle I \rangle^2$ and $\Delta_I^2 \equiv \langle I \rangle^2 / \langle I^2 \rangle_c$; for tube geometry $\Delta_I^2 \sim g_0$, while for slab geometry $\Delta_I^2 \sim Llk^2$, where k is the radiation wave vector (the intensity is measured on the output face). In Fig. 4 the intensity distribution function on the output face of the

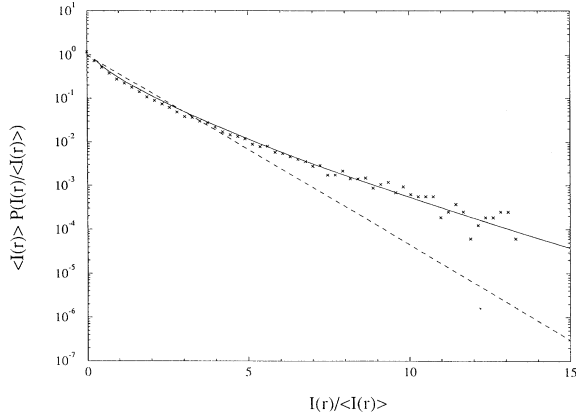


FIG. 4. Intensity distribution function in a semilogarithmic scale. The full line corresponds to Eq. (20), the dotted line to Rayleigh statistics, and the (+) symbols to the results of the numerical simulation.

sample is plotted. The full line corresponds to Eq. (20), while the dotted line corresponds to Rayleigh statistics and the (+) symbols to the results of the numerical simulation. Strong deviations of the simulation results from the Rayleigh distribution can be seen, especially in the tail region. On the other hand, an excellent fit with Eq. (20) is obtained.

For $I / \langle I \rangle \gg \Delta_I^2$ we get

$$P(I) \sim \exp \left[-\frac{3 I^{2/3}}{2 \langle I^2 \rangle_c^{1/3}} \right]. \quad (21)$$

This tail is close to what was obtained experimentally in Ref. 7.

For the intensity moments we have

$$\langle I^n \rangle = n! \left(\frac{\langle I \rangle}{2i\Delta_I} \right)^n H_n(i\Delta_I), \quad (22)$$

From Eq. (22) in the linear approximation with respect to Δ_I , we obtain

$$\langle I^n \rangle = n! \langle I \rangle^n [1 + n(n-1)/2\Delta_I^2]. \quad (23)$$

This dependence with respect to n was obtained by many different ways.^{9,10} In Ref. 10 there a simple qualitative explanation of the overshooting of fluctuations with respect to Rayleigh statistics based on the interference between intersecting trajectories was given.

In Fig. 5 are plotted the moments of the intensity at a given point. The full line corresponds to Eq. (22), the line coinciding with the abscissa corresponds to Rayleigh statistics and the (+) symbols to the results of the numerical simulation. Good agreement is obtained up to the 12th moment. It is interesting to note that the falloff of the high moments for the intensity at a given point occurs for higher moments than for the angular transmission coefficients.

It is interesting to see what topological perturbation theory means when applied to the conductance distribution function. This time, as follows from the definition of t_a , we would have to tackle the diagrams with n re-

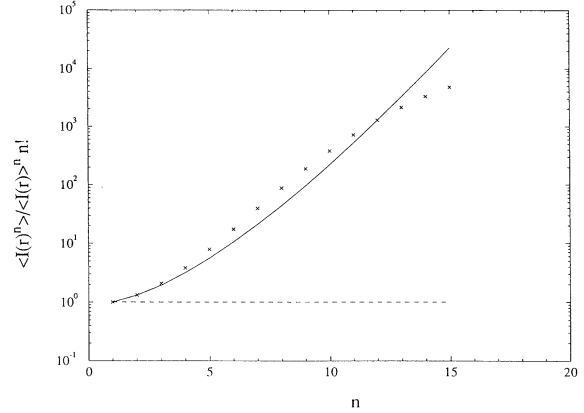


FIG. 5. Moments of the intensity in a given point in a semilogarithmic scale. The full line corresponds to Eq. (22), the line coinciding with the abscissa corresponds to Rayleigh statistics, and the (+) symbols to the results of the numerical simulation.

tarded propagators $G_{ab}^R, G_{a'b'}^R, \dots, G_{a^{(n)}b^{(n)}}^R$ and, respectively, n advanced propagators $G_{ab}^A, G_{a'b'}^A, \dots, G_{a^{(n)}b^{(n)}}^A$. We can again make the topological classification of diagrams. This time the situation is more complicated than previously because the propagators differ from each other, but we shall impose an additional selection principle. We shall consider as blocks for the connected diagrams only the pairs with coinciding propagators. That is, if the propagator $G_{a^{(i)}b^{(i)}}^R$ enters in some diagram, there should also enter the propagator $G_{a^{(i)}b^{(i)}}^A$; other diagrams, which do not fulfill this requirement, give for $\langle g^n \rangle$ a correction of higher order with respect to the parameter $1/N$, where $N = W^2 k^2$ is the number of transverse channels (W^2 is the area of the sample) due to the necessity of satisfying momentum conservation. Thus, we obtain the analog of Eq. (3):

$$\langle g^n \rangle = \sum_{m_1, m_2, \dots, m_n} P(m_1, m_2, \dots, m_n) \times \langle g \rangle_c^{m_1} \langle g^2 \rangle_c^{m_2} \dots \langle g^n \rangle_c^{m_n}, \quad (24)$$

where the connected diagram contribution $\langle g^i \rangle_c$ is the sum of all connected diagrams with i pairs of propagators. Therefore, we can immediately write down

$$P(g) = \int_{-\infty}^{\infty} \exp(i\zeta g) \exp \left(\sum_{n=1}^{\infty} \frac{(-i\zeta)^n}{n!} \langle g^n \rangle_c \right) \frac{d\zeta}{2\pi}. \quad (25)$$

Hence we have the very simple relation $\langle g^n \rangle_c = \langle \langle g^n \rangle \rangle$, where $\langle \langle g^n \rangle \rangle$ is the cumulant of the conductance distribution function. We see that for the conductance, the topological expansion is rather trivial; it simply coincides with the cumulant expansion (of course, this is definitely not the case for the angular transmission coefficient). In the first-order approximation, we would get no fluctuations at all; in the second-order approximation, we would get a Gaussian distribution function:

$$P(g) \sim \exp\left[-\frac{(g - \langle g \rangle)^2}{2\langle(\delta g)^2\rangle}\right]. \quad (26)$$

It was shown⁴ that

$$\langle\langle g^n \rangle\rangle \sim g_0^{2-n}. \quad (27)$$

Thus, at least for conductance we can claim that the topological expansion is simply an expansion with respect to $1/g_0$. This can also serve as a hint of what the parameter of expansion is when the topological perturbation theory is applied to the angular transmission coefficient (intensity) distribution function.

Since the diagrams for total transmission coefficient topologically equivalent to the diagrams for conductance, we can immediately deduce that

$$P(t_a)\{\langle t_a \rangle, \langle t_a^2 \rangle \cdots \langle t_a^m \rangle_c\} = P(g)\{\langle g \rangle, \langle g^2 \rangle \cdots \langle g^m \rangle_c\}. \quad (28)$$

One should understand Eq. (28) in the functional sense, i.e., the left-hand side is the same function of its arguments as the right-hand side. Therefore for the total transmission coefficient in the first-order approximation, we would get no fluctuations at all, and in the second-order approximation, we would get the Gaussian distribution function,

$$P(t_a) \sim \exp\left[-\frac{(t_a - \langle t_a \rangle)^2}{2\langle(\delta t_a)^2\rangle}\right], \quad (29)$$

or equivalently for the moments

$$\langle t_a^n \rangle = \langle t_a \rangle^n \sum_{m=0}^{[n/2]} \frac{n!}{m!(n-2m)!} \left(\frac{\langle t_a^2 \rangle_c}{2\langle t_a \rangle^2}\right)^m. \quad (30)$$

In Fig. 6 we plot the moments of the total transmission. The full line represents the Gaussian distribution given by Eq. (30), while the (+) symbols are the results of our simulation. A good fit up to the eighth moment can be seen.

In conclusion, general topological approximations were formulated for the angular transmission coefficient and intensity distribution functions. We show that Rayleigh statistics for the angular transmission coefficients (intensity) correspond to the first-order approximation and we calculate explicitly the statistics in the second-order approximation. It is shown that only for small values of the argument are the distribution functions for intensity radiated in a given direction or in a given point in a random medium [$P(t_{ab})$ and $P(I)$] given by simple exponentials, as predicted by Rayleigh statistics. For larger values the distribution functions differ drastically from simple exponentials, and the asymptotic behavior is a stretched exponential. The results obtained were confirmed by numerical simulations.

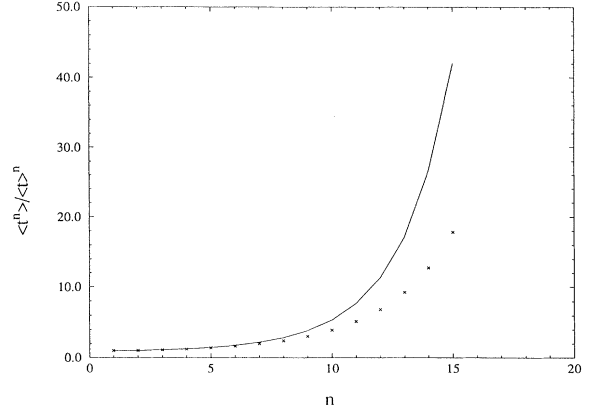


FIG. 6. Moments of the total transmission. The full line represents the Gaussian distribution given by Eq. (30), and the (+) symbols are the results of our simulation.

APPENDIX

Instead of the integral representation of Eq. (7), we may use a more general integral representation for $n!$:

$$n! = k^{n+1} \int_0^\infty du u^n \exp(-ku), \quad \text{Re } k > 0, \quad (A1)$$

where k will be determined later. Then for the distribution function $P(t_{ab})$ we have, changing the integration variable to $\zeta = \xi u$:

$$\begin{aligned} P(t_{ab}) &= \int_{-\infty}^\infty \exp(i\zeta t_{ab}/u) \\ &\times \int_0^\infty du \sum_{n=0}^\infty \frac{(-ik\zeta)^n}{n!} M_n \frac{1}{u} \\ &\times \exp(-ku) k \frac{d\zeta}{2\pi}. \end{aligned} \quad (A2)$$

Instead of Eqs. (10) and (11) we finally obtain:

$$P(t_{ab}) = \int_0^\infty dv \tilde{P}(k, v) \frac{1}{v} \exp\left(-\frac{kt_{ab}}{v}\right) \quad (A3)$$

and

$$\begin{aligned} \tilde{P}(k, v) &= \int_{-\infty}^\infty \exp(i\zeta v) \\ &\times \exp\left(\sum_{n=1}^\infty \frac{(-ik\zeta)^n}{n!} \langle t_{ab}^n \rangle_c\right) k \frac{d\zeta}{2\pi}. \end{aligned} \quad (A4)$$

Choosing $k = 1$, we obtain Eqs. (10) and (11). For a given approximation, k should be chosen in such a way to procure a correct sign before the highest power of ζ in the reduced exponent and hence the convergence of the integration with respect to $d\zeta$ in Eq. (A4).

¹P. A. Lee and A. D. Stone, Phys. Rev. Lett. **55**, 1623 (1985).

²B. L. Altshuler, Pis'ma Zh. Eksp. Teor. Fiz. **51**, 530 (1981) [JETP Lett. **41**, 648 (1981)].

³S. Feng, C. L. Kane, P. A. Lee, and A. D. Stone, Phys. Rev.

Let. **61**, 834 (1988).

⁴B. L. Altshuler, V. E. Kravtsov, and I. V. Lerner, in *Mesoscopic Phenomena in Solids*, edited by B. L. Altshuler, P. A. Lee, and R. A. Webb (North-Holland, Amsterdam, 1991).

⁵A. Z. Genack and N. Garcia, *Europhys. Lett.* **21**, 753 (1993).

⁶B. Shapiro, *Phys. Rev. Lett.* **57**, 2168 (1986).

⁷N. Garcia and A. Z. Genack, *Phys. Rev. Lett.* **63**, 1678 (1989).

⁸The convergence radius of the series may be improved by

using Padé approximants.

⁹R. Dashen, *J. Math. Phys.* **20**, 894 (1979).

¹⁰N. Shnerb and M. Kaveh, *Phys. Rev.* **43**, 1279 (1991).

¹¹I. Edrei, M. Kaveh, and B. Shapiro, *Phys. Rev. Lett.* **62**, 2120 (1989).